MATERIALS PHYSICS AND MECHANICS RESEARCH ARTICLE

Submitted: July 16, 2025 Revised: July 29, 2025 Accepted: August 22, 2025

Landau–Lifshitz–Gilbert equation: magnetization of a superparamagnetic particle ensemble in the mean-field approximation

P.V. Kharitonskii [1,2] ✉, N.A. Ivanov [2], L.I. Guzilova [1], K.G. Gareev [1,2]

[1] Ioffe Institute, St. Petersburg, Russia

[2] St. Petersburg Electrotechnical University "LETI", St. Petersburg, Russia

✉ peterkh@yandex.ru

ABSTRACT

A numerical method for solving the Landau–Lifshitz–Gilbert equation for an ensemble of superparamagnetic nanoparticles within the mean-field approximation is presented. The classical fourth-order Runge–Kutta method is employed for the time integration of the equation. The model simulates an ensemble of uniaxial nanoparticles subjected to a constant external magnetic field. It is shown that the proposed approach accurately reproduces the magnetization dynamics: the components perpendicular to the field decay, while the longitudinal component relaxes toward a steady-state value. The results are qualitatively consistent with previously published data obtained using the *Vinamax* simulation software.

KEYWORDS

superparamagnetism • diluted magnet • Landau–Lifshitz–Gilbert equation • mean-field approximation dipole–dipole interaction

Citation: Kharitonskii PV, Ivanov NA, Guzilova LI, Gareev KG. Landau–Lifshitz–Gilbert equation: magnetization of a superparamagnetic particle ensemble in the mean-field approximation. *Materials Physics and Mechanics.* 2025;53(4): 91–98.

http://dx.doi.org/10.18149/MPM.5342025_7

Introduction

Within the framework of micromagnetic theory, a magnet is treated as a mesoscopic medium, in which atomic-scale structural features can be neglected [1]. The magnetic properties of magnetically ordered materials (magnets) are governed by the presence of intrinsic or induced internal magnetic ordering. In the context of the continuum model, this ordering can be represented as a spatial distribution of the macroscopic magnetization per unit volume $\mathbf{M}(\mathbf{r},t)$. The dynamics of the magnetization vector is described by the Landau–Lifshitz–Gilbert (LLG) equation, which accounts for both gyromagnetic effects and dissipative processes. The objective of this study is to perform numerical simulations of magnetization dynamics in systems containing a large number of superparamagnetic particles, within the mean-field approximation of dipole–dipole interactions between them [2–5].

Method for solving the LLG equation

For small single-domain particles, where the magnetization can be considered spatially uniform, the macrospin approximation is applied. The magnetization dynamics of the i-th particle is described by an equation that, taking into account the normalization of the magnetization vector, reads as follows $\mathbf{m} = \mathbf{M}/I_s$ (I_s is the spontaneous magnetization) takes the form [6]:

$$\frac{\partial \mathbf{m}^{(i)}}{\partial t} = -\gamma \mathbf{m}^{(i)} \times \mathbf{H}_{eff}^{(i)} + \alpha \mathbf{m}^{(i)} \times \frac{\partial \mathbf{m}^{(i)}}{\partial t}, \quad (1)$$

where γ is the gyromagnetic ratio, α is the dimensionless Gilbert damping parameter; $\mathbf{H}_{eff}$ is the effective field acting on the magnetization of the *i*-th particle. The effective field is defined as:

$$\mathbf{H}_{eff}^{(i)} = -\frac{1}{I_s}\frac{\partial U^{(i)}}{\partial \mathbf{m}^{(i)}}, \quad (2)$$

where $U^{(i)}$ is the total energy density (energy per unit volume) of the *i*-th particle.

The total energy density of the *i*-th particle can be written as:

$$U^{(i)} = U_{ext}^{(i)} + U_{anis}^{(i)} + U_d^{(i)}. \quad (3)$$

Here, U_{ext} is the energy in the external field, U_{anis} is the magnetocrystalline anisotropy energy, U_d is the dipole–dipole interaction energy:

$$U_{ext}^{(i)} = -I_s \mathbf{m}^{(i)} \cdot \mathbf{H}_{ext}, \quad (4)$$

$$U_{anis}^{(i)} = K_u\left(1 - \left(\mathbf{m}^{(i)} \cdot \mathbf{e}_u^{(i)}\right)^2\right), \quad (5)$$

$$U_d^{(i)} = -\frac{1}{2} I_s \mathbf{m}^{(i)} \cdot \mathbf{H}_d. \quad (6)$$

In equations (4)–(6), the following notations are used: $\mathbf{H}_{ext}$ is the external magnetic field, K_u is the effective anisotropy constant, $\mathbf{e}_u$ is the unit vector along the uniaxial anisotropy direction of the particle, $\mathbf{H}_d$ is the dipole–dipole interaction field (demagnetizing field).

Accurate evaluation of dipole–dipole interactions remains the principal computational bottleneck in micromagnetic modelling. A brute-force summation of all pairwise interactions require $O(N^2)$ operations for a system of *N* magnetic moments [7]. Two acceleration strategies are now most widely employed: the fast multipole method (FMM) [8–11] and convolution techniques that exploit the fast Fourier transform (FFT) [12–14]. Both approaches reduce the complexity to $O(N\log N)$ while maintaining controllable accuracy. Modern hybrid solvers such as *FastMag* [15] merge FMM or FFT kernels with finite-difference or finite-element discretization and leverage multi-GPU hardware to simulate systems containing up to ~ 10^8 computational cells. Further gains can be realized by re-using the demagnetizing field within multi-stage time integrators through polynomial extrapolation, roughly halving the wall-time of explicit schemes without compromising precision [16]. Despite these advances, current computational resources still limit routine simulations to ensembles of only a few million interacting moments, underscoring the need for new, more scalable algorithms capable of bridging the gap to truly device–scale problems.

According to Eq. (2)–(6), the effective field acting on the magnetization of the *i*-th particle is defined as:

$$\mathbf{H}_{eff}^{(i)} = \mathbf{H}_{ext} + \frac{2K_u}{I_s}\left(\mathbf{m}^{(i)} \cdot \mathbf{e}_u^{(i)}\right)\mathbf{e}_u^{(i)} + \frac{1}{2}\mathbf{H}_d. \quad (7)$$

In this study, the magnetic material is modeled as an ensemble of dipole–dipole interacting superparamagnetic solid spheres with diameter d_0 and volume $V^{(i)}$, each possessing uniaxial anisotropy. The particles are uniformly distributed and fixed within a nonmagnetic matrix shaped as a cylinder of height *d* and radius *R*. The external magnetic field $\mathbf{H}_{ext}$ is applied along the *Oz*-axis, which is aligned with the cylinder's generatrix.

To accurately model superparamagnetic systems, it is essential to account for the influence of thermal fluctuations on the magnetization dynamics. A stochastic term can be introduced into Eq. (1) to describe the effect of thermal fluctuations at nonzero temperature $T \neq 0$. The resulting equation for the i-th particle takes the following form:

$$\frac{\partial \mathbf{m}^{(i)}}{\partial t} = -\gamma \mathbf{m}^{(i)} \times \mathbf{H}^{*(i)}_{eff} + \alpha \mathbf{m}^{(i)} \times \frac{\partial \mathbf{m}^{(i)}}{\partial t}, \tag{8}$$

$$\mathbf{H}^{*(i)}_{eff} = \mathbf{H}^{(i)}_{eff} + \mathbf{H}^{(i)}_{therm}. \tag{9}$$

Here $\mathbf{H}^{(i)}_{therm}$ is the stochastic thermal field [17–23], modeled as a Gaussian random process with zero mean and a correlation function that satisfies the fluctuation–dissipation theorem. The stochastic thermal field acting on the i-th particle can be expresses as [24–26]:

$$\mathbf{H}^{(i)}_{therm} = \boldsymbol{\eta}^{(i)} \sqrt{\frac{2\alpha k_B T}{\gamma I_s V^{(i)} \Delta t}}, \tag{10}$$

where $\boldsymbol{\eta}^{(i)}$ is a vector, whose components are normally distributed random variables with zero mean, uncorrelated in both space and time; k_B is the Boltzmann constant, Δt is the time step.

Within the framework of the considered model, the components of the effective field acting on the magnetization of the i-th particle in the Cartesian coordinate system are defined as:

$$\mathbf{H}_{ext} = (0, 0, H_0), \tag{11}$$

where H_0 is the magnitude of the external magnetic field.

The components of the magnetocrystalline anisotropy field are then given by:

$$\begin{cases} H^{(i)}_{anis,x} = \frac{2K_u}{I_s}\left(\mathbf{m}^{(i)} \cdot \mathbf{e}^{(i)}_u\right) e^{(i)}_x, \\ H^{(i)}_{anis,y} = \frac{2K_u}{I_s}\left(\mathbf{m}^{(i)} \cdot \mathbf{e}^{(i)}_u\right) e^{(i)}_y, \\ H^{(i)}_{anis,z} = \frac{2K_u}{I_s}\left(\mathbf{m}^{(i)} \cdot \mathbf{e}^{(i)}_u\right) e^{(i)}_z, \end{cases} \tag{12}$$

where e_x, e_y, e_z are the components of the unit vector along the uniaxial anisotropy axis.

To account for the influence of dipole–dipole interactions between particles in the ensemble, this work proposes the use of a mean-field method based on the statistical approach developed in [2]:

$$H_{d,z} = -\frac{8\pi}{3} c I_s \left(1 - \frac{3}{2}\cos\theta_{max}\right)\zeta, \tag{13}$$

$$\zeta = \sum_{i=1}^{N} m^{(i)}_z, \tag{14}$$

where c is the volume concentration of particles, θ_{max} is the maximum angle between the position vector of a particle and the Oz-axis of the cylinder, ζ is the dimensionless magnetization of the ensemble. The use of this method reduces the computational complexity to $O(N)$.

Equation (1) for i-th particle in the Cartesian coordinate system is written as:

$$\begin{cases} \frac{\partial m_x}{\partial t} = -\frac{\gamma}{1+\alpha^2}\left[(m_y + \alpha m_x m_z)H_{eff,z} - (m_z - \alpha m_y m_x)H_{eff,y} - \alpha(m_y^2 + m_z^2)H_{eff,x}\right], \\ \frac{\partial m_y}{\partial t} = -\frac{\gamma}{1+\alpha^2}\left[(m_z + \alpha m_y m_x)H_{eff,x} - (m_x - \alpha m_z m_y)H_{eff,z} - \alpha(m_z^2 + m_x^2)H_{eff,y}\right], \\ \frac{\partial m_z}{\partial t} = -\frac{\gamma}{1+\alpha^2}\left[(m_x + \alpha m_z m_y)H_{eff,y} - (m_y - \alpha m_x m_z)H_{eff,x} - \alpha(m_x^2 + m_y^2)H_{eff,z}\right]. \end{cases} \tag{15}$$

When thermal fluctuations are taken into account, the components $\mathbf{H}^{(i)}_{eff}$ in Eq. (15) are replaced with the components $\mathbf{H}^{*(i)}_{eff}$ in accordance with Eq. (9).

To integrate the resulting system of equations ($3N$ first-order ordinary differential equations for N particles), the classical explicit fourth-order Runge–Kutta method [27–29] was employed with a time step of 10^{-12} s, which satisfies the stability criterion. After each integration step, the magnetization vector $\mathbf{m}^{(i)}$ was renormalized to ensure that the condition $|\mathbf{m}^{(i)}| = 1$ is maintained [30].

Results and Discussion

In the numerical experiments, parameters in the CGS unit system were used, corresponding to the magnetic material described in [31] with the damping parameter α chosen according to [24]. The characteristics are listed in Table 1.

Table 1. Key parameters used in the simulation

Parameter	**Value**
Saturation magnetization I_s, emu/cm^3	480
Anisotropy constant K_u, erg/cm^3	135000
Particle diameter d_0, cm	10^{-6}
Cylinder height d, cm	10^{-4}
Cylinder radius R, cm	$0.5 \cdot 10^{-4}$
Volume concentration c	0.3
Damping parameter α	0.1
External magnetic field H_0, Oe	100...600

The easy axes of magnetization of the particles were uniformly distributed along the six coordinate directions ($\pm x$, $\pm y$, $\pm z$), with one-sixth of the particles assigned to each direction, thereby ensuring an initially demagnetized state of the ensemble. As the initial condition, the magnetization of each particle was aligned with its easy axis. The LLG equations were then solved for all particles until a steady-state configuration was reached.

The result of numerical modeling of the magnetization dynamics of the i-th particle, whose easy axis is aligned along the x-axis, in an ensemble of superparamagnetic particles at $T = 0$ K and $H_0 = 600$ Oe is shown in Fig. 1. Figure 2 presents the results for the averaged magnetization vector of the ensemble.

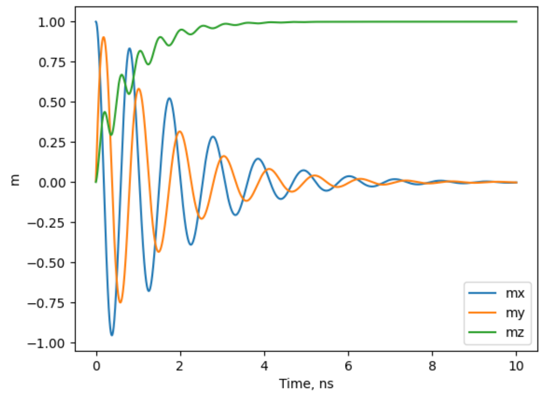

Fig. 1. Time dependence of the components of the normalized magnetization vector of the i-th particle with its easy axis aligned along the x-axis, at $T = 0$ K and $H_0 = 600$ Oe

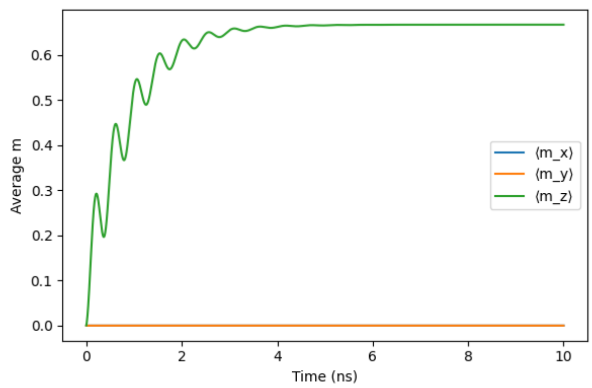

Fig. 2. Time dependence of the components of the ensemble-averaged magnetization at $T = 0$ K and $H_0 = 600$ Oe

The obtained results (Fig. 1) demonstrate the relaxation of m_z toward an equilibrium state and the gradual decay of m_x and m_y. This behavior illustrates the Gilbert damping mechanism and indicates the correct implementation of both anisotropy and dipolar fields within the mean-field approximation. To verify the model, the results were compared with those obtained using *Vinamax* [24], a macrospin simulator that accounts for similar physical effects. The comparison showed qualitative agreement, confirming the physical validity and applicability of the proposed method.

To account for thermal effects in the simulations, Eq. (10) was used, with the vector $\boldsymbol{\eta}^{(i)}$ updated at each time step. The results of numerical modeling of the magnetization dynamics of the *i*-th particle, whose easy axis is aligned along the *x*-axis, in an ensemble of superparamagnetic particles at T = 300 K and for H_0 equal to 100, 200 and 300 Oe are presented in Figs. 3, 4, and 5, respectively.

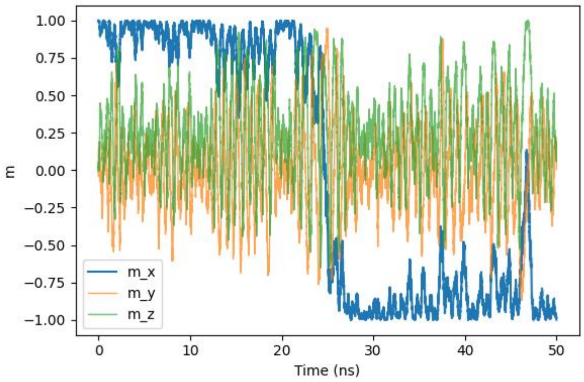

Fig. 3. Time dependence of the components of the normalized magnetization vector of the *i*-th particle with its easy axis aligned along the *x*-axis, at T = 300 K and H_0 = 100 Oe

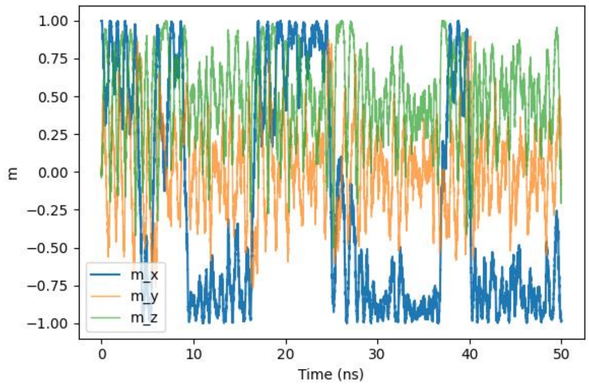

Fig. 4. Time dependence of the components of the normalized magnetization vector of the *i*-th particle with its easy axis aligned along the *x*-axis, at T = 300 K and H_0 = 200 Oe

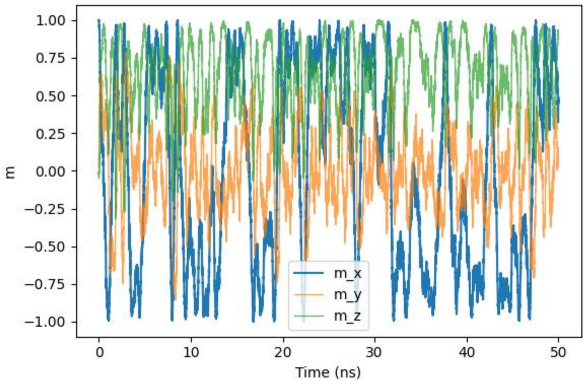

Fig. 5. Time dependence of the components of the normalized magnetization vector of the *i*-th particle with its easy axis aligned along the *x*-axis, at T = 300 K and H_0 = 300 Oe

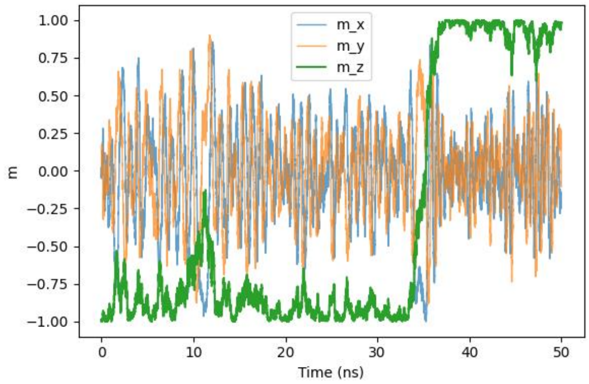

Fig. 6. Time dependence of the components of the normalized magnetization vector of the *i*-th particle with its easy axis oriented opposite to the *z*-axis, at T = 300 K and H_0 = 100 Oe

The results of numerical modeling of the magnetization dynamics of the *i*-th particle, whose easy axis is aligned along the negative *z*-axis, in an ensemble of superparamagnetic particles at T = 300 K and for H_0 equal to 100, 200 and 300 Oe are presented in Figs. 6, 7, and 8, respectively.

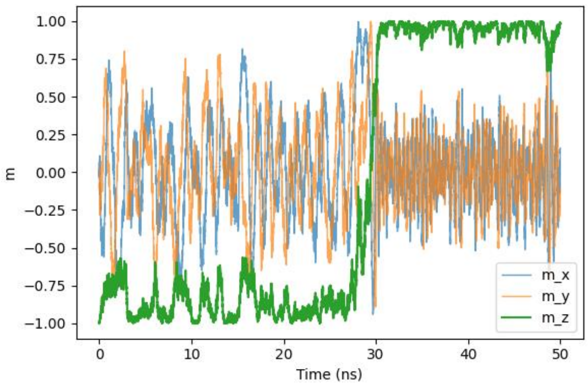

Fig. 7. Time dependence of the components of the normalized magnetization vector of the *i*-th particle with its easy axis oriented opposite to the *z*-axis, at T = 300 K and H_0 = 200 Oe

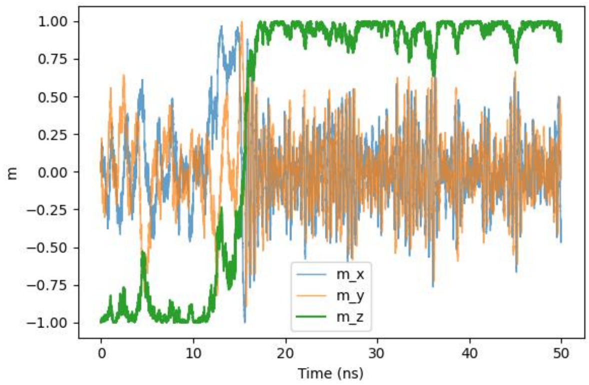

Fig. 8. Time dependence of the components of the normalized magnetization vector of the *i*-th particle with its easy axis oriented opposite to the *z*-axis, at T = 300 K and H_0 = 300 Oe

Analysis of the time dependencies of the magnetization vector components (Figs. 3–8) shows that, under the condition $T > 0$, bistable behavior is observed along the easy anisotropy axis, which is consistent with the classical theory of superparamagnetism. As the magnitude of the external magnetic field increases, the degree of alignment of the magnetic moments along the field direction also increases.

Conclusions

In the study, a numerical method for simulating the dynamics of an ensemble of dipole–dipole interacting superparamagnetic nanoparticles based on the Landau–Lifshitz–Gilbert equation with thermal fluctuations has been proposed and implemented. To describe interparticle interactions, a mean-field approximation was employed, which significantly reduces computational cost.

The integration of the system of equations was carried out using the explicit fourth-order Runge–Kutta method, which ensures numerical stability and accuracy at a small-time step (time step 10^{-12} s). Numerical experiments performed for a diluted ensemble (c = 0.3) of uniaxial superparamagnetic nanoparticles demonstrated that the model accurately captures the relaxation processes: decay of the transverse components of the magnetization vector and convergence of the longitudinal component to an equilibrium state. Comparison with results obtained using the specialized simulation software *Vinamax* [24] confirms the physical validity of the proposed approach.

The simulation results at both zero and room temperature are consistent with classical concepts of superparamagnetism, including bistability along the easy anisotropy axis and enhanced alignment of magnetic moments with increasing external magnetic field strength.

Thus, the proposed method, in combination with the macrospin approximation and the inclusion of thermal fluctuations in the Landau–Lifshitz–Gilbert equation, can be effectively used for numerical analysis of collective magnetic dynamics in diluted magnets composed of superparamagnetic nanoparticles. From the point of view of practical application of the obtained results, a detailed understanding of the magnetization dynamics of structures containing iron oxide in the form of micro- and nanosized particles can be useful in the development of new generation materials designed to protect against the effects of microwave electromagnetic radiation [32].

CRediT authorship contribution statement

Peter V. Kharitonskii: writing – review & editing, conceptualization; **Nikolai A. Ivanov**: investigation, writing – original draft; **Liubov I. Guzilova**: writing – review & editing; **Kamil G. Gareev**: supervision, writing – review & editing.

Conflict of interest

The authors declare that they have no conflict of interest.

References

1. Coey JMD. *Magnetism and magnetic materials.* Cambridge: Cambridge University Press; 2010.
2. Kharitonskii PV, Setrov EA, Ralin AY. Modeling of hysteresis characteristics of a dilute magnetic with dipole–dipole interaction of particles. *Materials Physics and Mechanics.* 2024;52(2): 142–150.
3. Sánchez FH, Mendoza Zélis P, Arciniegas ML, Pasquevich GA, Fernández van Raap MB. Dipolar interaction and demagnetizing effects in magnetic nanoparticle dispersions: introducing the mean-field interacting superparamagnet model (MFISP Model). *Physical Review B.* 2017;95: 134421.
4. Landi GT. The random dipolar-field approximation for systems of interacting magnetic particles. *Journal of Applied Physics.* 2013;113: 163908.
5. Sánchez FH, Mendoza Zélis P, Arciniegas ML, Pasquevich GA, Fernández van Raap MB. Dipolar interaction and demagnetizing effects in magnetic nanoparticle dispersions: introducing the mean-field interacting superparamagnet model. *Physical Review B.* 2017;95(13): 134421.
6. Gilbert TL. A phenomenological theory of damping in ferromagnetic materials. *IEEE Transactions on Magnetics.* 2004;40(6): 3443–3449.
7. Izotov AV, Belyaev BA, Valikhanov MM, Polenga SV, Stefanyuk AV. Algorithm for calculating the equilibrium state of a ferromagnet based on the Lagrange-multiplier method. *Computational Methods and Programming.* 2012;13(4): 551–559. (In Russian)
8. Greengard L, Rokhlin V. A fast algorithm for particle simulations. *Journal of Computational Physics.* 1987;73(2): 325–348.
9. Zipunova EV, Ivanov AV. On calculation of the demagnetizing field by the fast multipole method. *Preprints of the Keldysh Institute of Applied Mathematics.* 2018;140: 19. (In Russian)
10. Tan X, Baras JS, Krishnaprasad PS. Fast evaluation of demagnetizing field in three-dimensional micromagnetics using multipole approximation. In: Varadan VV. (eds.) *Proc. SPIE 3984, Smart Structures and Materials 2000: Mathematics and Control in Smart Structures, (19 June 2000).* SPIE; 2000. p.195-201.
11. Zhang W, Haas S. Adaptation and performance of the Cartesian coordinates fast multipole method for nanomagnetic simulations. *Journal of Magnetism and Magnetic Materials.* 2009;321(22): 3687–3692.
12. Moutinho JPG. *Micromagnetic device simulation.* Lisbon: Instituto Superior Técnico, Universidade de Lisboa; 2017.
13. Fredkin DR, Koehler TR. Hybrid method for computing demagnetizing fields. *IEEE Transactions on Magnetics.* 1990;26(2): 415–417.
14. Long HH, Ong ET, Liu ZJ, Li EP. Fast Fourier transform on multipoles for rapid calculation of magnetostatic fields. *IEEE Transactions on Magnetics.* 2006;42(2): 295–300.
15. Chang R, Li S, Lubarda MV, Livshitz B, Lomakin V. FastMag: fast micromagnetic solver for large-scale simulations. *CMRR Report.* 2010;34: 16.
16. Lepadatu S. Speeding up explicit numerical evaluation methods for micromagnetic simulations using demagnetizing field polynomial extrapolation. *IEEE Transactions on Magnetics.* 2022;58(5): 1–16.
17. Brown WF. Thermal fluctuations of a single-domain particle. *Physical Review.* 1963;130(5): 1677–1686.
18. García-Palacios JL, Lázaro FJ. Langevin-dynamics study of the dynamical properties of small magnetic particles. *Physical Review B.* 1998;58: 14937–14958.

19. Coffey WT, Kalmykov YuP. Thermal fluctuations of magnetic nanoparticles: Fifty years after Brown. *Journal of Applied Physics.* 2012; 112: 121301.
20. Durhuus FL, Beleggia M, Frandsen C. Conservation laws for interacting magnetic nanoparticles at finite temperature. *Physical Review B.* 2024;109(5): 054421.
21. Coffey WT, Kalmykov YuP, Waldron JT. *The Langevin equation: with applications to stochastic problems in physics, chemistry and electrical engineering.* 2nd ed. Singapore: World Scientific; 2004.
22. Brzuszek K, Ross CA, Janutka A. High-frequency magnetic response of superparamagnetic composites of spherical $Fe_{65}Co_{35}$ nanoparticles. *Journal of Magnetism and Magnetic Materials.* 2023;573: 170651.
23. Berkov DV. Magnetization dynamics including thermal fluctuations: basic phenomenology, fast remagnetization processes and transitions over high-energy barriers. In: Kronmüller H, Parkin S. (eds.) *Handbook of Magnetism and Advanced Magnetic Materials.* Vol. 2: Micromagnetism. Chichester: John Wiley & Sons; 2007. 795–823.
24. Leliaert J, Vansteenkiste A, Coene A, Dupré L, Van Waeyenberge B. Vinamax: a macrospin simulation tool for magnetic nanoparticles. *Medical & Biological Engineering & Computing.* 2015;53(2): 309–317.
25. Vansteenkiste A, Leliaert J, Dvornik M, Helsen M, Garcia-Sanchez F, Van Waeyenberge B. The design and verification of MuMax3. *AIP Advances.* 2014;4(10): 107133.
26. Frantiu MA. *Micromagnetic simulations of magnetic thin films using MuMax3. Bachelor's thesis.* Groningen: University of Groningen; 2019.
27. Gorelov YuN, Kurganskaya LV. *Numerical methods for solving ordinary differential equations (Runge-Kutta method): textbook.* Samara: Samara University Press; 2023. (In Russian)
28. Liu C, Ku Y. A combination of group preserving scheme and Runge-Kutta method for the integration of Landau-Lifshitz equation. *Computer Modeling in Engineering & Sciences.* 2005;9(2): 151–178.
29. Shiach J. Advanced ordinary differential equations & dynamical systems: Runge-Kutta methods. *Online Lecture Notes.* 2020.
30. Botha AE. Stabilisation of the Landau-Lifshitz-Gilbert equation for numerical solution via standard methods. *Scientific Reports.* 2025;15: 15775.
31. Kharitonskii P, Bobrov N, Gareev K, Kosterov A, Nikitin A, Ralin A, Sergienko E, Testov O, Ustinov A, Zolotov N. Magnetic granulometry, frequency-dependent susceptibility and magnetic states of particles of magnetite ore from the Kovdor deposit. *Journal of Magnetism and Magnetic Materials.* 2022;553: 169279.
32. Boiprav OV, Pevneva NA, Ayad H. Development and study of multilayer electromagnetic radiation shields based on powdered oxide-containing materials. *Materials Physics and Mechanics.* 2021;47(1): 123–130.